Blind Source Separation Spectrum Detection Method Based on Wavelet Transform and Singular Spectrum Analysis

Qian Hu, Zhongqiang Luo, and Wenshi Xiao

***Abstract*—To address the issue of reduced detection performance due to the impaired separation mechanism affected by noise, this paper proposes a blind source separation (BSS) detection method based on Wavelet Transform (WT) and Singular Spectrum Analysis (SSA). Firstly, the input signal is denoised using WT. Then, SSA is employed to denoise and reduce the dimension of the processed signal. Subsequently, the independent component analysis (ICA) based BSS algorithm is employed to separate the mixed signal preprocessed by the previous two ways. Finally, the proposed algorithm and the BSS detection method based on WT are compared in terms of spectrum analysis and separation performance. Simulation results show that the blind source separation detection method based on WT-SSA has a better signal detection performance.**

***Index Terms*—blind source separation; wavelet transform; singular spectrum sensing; independent component analysis**

I. INTRODUCTION

IN WIRELESS communication environments, the wireless channels are always complex, so that transmitting signals will be affected by channel fading and noise, resulting in mixed signals at the receiving end, and most detection algorithms such as traditional energy detection algorithms are unable to distinguish mixed signals to implement spectrum detection. Therefore, blind source separation is an often used promising method for solving this problem thanks to its advanced technical superiority [1][2][3]. Blind source separation refers to the analysis of the unobserved original signal from multiple observed mixed signals. Usually the observed mixed signals come from the outputs of multiple sensors and the output signals of the sensors are independent. Blind source separation has received a great deal of attention as a comprehensive research field that intersects with information theory, signal processing, artificial neural networks, probability theory, and other disciplines. In recent years, blind signal processing has become an important development direction in many research areas such as modern digital signal processing and computational intelligence, and it has great potential for applications in electronic information technology, communications, biomedicine, image enhancement, radar systems, geophysical signal processing and other fields. Blind signal processing relies on the statistical properties of the source signal, and its study has always been a focus of researchers, with blind signal separation being one of the most important research topics. The meaning of "blind" is twofold: on the one hand, the source signal is not known; on the other hand, the source signal mixing method is also not known.

One of the most famous blind source separation algorithms is Independent Component Analysis (ICA). And there have sprung up many algorithms to improve on ICA for theory updates. In [4], the authors designed a fast Power Iterative Independent Component Analysis (PowerICA) noise suppression scheme based on power iteration. First, a single-channel blind separation model is transformed into a multichannel observation model by constructing a pseudo-observation signal through a weighting process. This blind separation algorithm is then used to separate the noise from the source signal. Finally, the effectiveness of the algorithm is verified by experimental simulation. In [5], the authors treat the Lagrange multiplier as a constant in the original derivation of the FastICA algorithm and use a temporary approximation to the Jacobi matrix in the Newton-Raphson update, and then provide an alternative derivation of the FastICA algorithm that does not require an approximation. Based on this, the authors propose a new FastICA power iteration algorithm that is more stable than the fixed-point algorithm when the sample size is not several orders of magnitude larger than the dimensionality. In [6], when the ICA model does not forget to hold in full, the real data used for simulation experiments are not accurate in completing the maximization of the corresponding likelihood. To address this situation, the authors proposed a new algorithm called Picard, which uses only the sparse approximation Hessian as a preprocessor for the L-BFGS algorithm, refining the Hessian approximation from the memory of past iterations. The results demonstrate the superior performance of the proposed technique, especially on real data, by comparing a wide range of values for several algorithms of the same class through simulations.

The algorithms mentioned above in the literature are only a small part of the blind source separation algorithms, but all of them have proved the effectiveness of blind source separation. As the presence of factors such as noise in complex wireless communication environments can affect the effectiveness of signal separation, it is necessary to denoise and reduce the signal dimension prior to implementing blind source separation. In this paper, the Wavelet Transform (WT) is first used for denoising, and then the Singular Spectrum Analysis (SSA) is used for denoising and reducing the dimension. These two methods are applied in many aspects, for example, in [7], the authors investigated the threshold selection problem in the

Qian Hu, Zhongqiang Luo, and Wenshi Xiao are with School of Automation and Information Engineering, Sichuan University of Science and Engineering, Yibin, China; Zhongqiang Luo is also with Intelligent Perception and Control Key Laboratory of Sichuan Province, Sichuan University of Science and Engineering, Yibin, China.

The corresponding author is Zhongqiang Luo (e-mail: luozhongqiang@suse.edu.cn)

DOI: 10.36244/ICJ.2025.4.6

image denoise process based on WT, the wavelet coefficients are obtained by WT of the image signal, suitable threshold values are selected to process the wavelet coefficients, and then the processed wavelet coefficients are inverted by WT to obtain the reconstructed denoised image. Simulation experiments prove that the adaptive threshold denoising technique based on WT has the best denoising result, which can clearly retain the details in the image without sharpening and oversmoothing, and its values of Signal-to-Noise Ratio (SNR) and peak SNR are the largest and the value of mean square error is the smallest, thus improving the overall quality of the image. In [8], the authors used a noise reduction method combining wavelet thresholding and Singular Value Decomposition (SVD) processing, and conducted a study on noise suppression of one-dimensional audio signals received by intelligent navigation for automotive noise pollution, and proposed a joint WT-SVD model algorithm, and finally, through simulated experimental comparison and analysis, the algorithm has good noise suppression for the received signals of intelligent navigation systems under the environment of automotive noise interference adaptive and good suppression performance. In [9], the authors studied the video electromagnetic leakage problem, first of all, the intercepted video electromagnetic leakage signal through the SSA method for noise reduction of the noisy video electromagnetic leakage signal, through simulation experiments found that the singular spectrum analysis method applied to the video electromagnetic leakage signal denoising not only to remove the noise relatively clean, and can well retain the original video electromagnetic signal details and features, The SNR is improved significantly. The above-mentioned papers have demonstrated that WT and SSA have good performance in noise removal, so this paper starts to study this.

From the above-mentioned paper, it can be seen that WT in image processing denoising effect is better, and in the wireless communication environment, the transmission signal will be mixed with the white noise present in the channel, at this time the wavelet denoising effect is not very satisfactory, and the SSA can be used by decomposing the signal into different components, and then according to certain rules, select certain effective components and reconstruct the new signal, to achieve the signal denoising and reducing the signal dimension[10] [11][12]. Based on this, this paper proposes a blind spectrum detection method based on WT and SSA, firstly using WT to denoise the received mixed signal, then using SSA to denoise and reduce the dimension of the processed signal again, and finally using the ICA_p algorithm in blind source separation to separate the mixed signal. The experimental results corroborate the effectiveness of the proposed scheme.

II. SYSTEM MODEL

In wireless communication systems, the situation in the channel is complex and variable, and the observed signals received at the receiver may be affected by noise or mixed with other signals, and many algorithms are unable to distinguish between the mixing sequences, so blind source separation is investigated. Blind source separation is a technique for separating independent source signals from a set of sensor measurements using only the weakly known condition that the source signals are independent of each other, given that the transfer function of the system, the mixing coefficients of the source signals and their probability distribution are unknown.

Assuming that there are m signals that are independent of each other and the length of these signals is T, after channel gain of A and an additive Gaussian white noise channel, a mixed received signal is obtained , i.e. the observed signal

$$X = AS + N. \tag{1}$$

Where A is the $m \times m$ mixing matrix, S is the *m*-dimensional original signal vector, N is the m -dimensional noise vector and X is the *m*-dimensional mixed signal vector, the expressions are as follows

$$S = [s_1, s_2, ..., s_m]. \tag{2}$$

$$N = [n_1, n_2, ..., n_m]. \tag{3}$$

$$X = [x_1, x_2, ..., x_m]. \tag{4}$$

Where $s_i, i = 1, 2, ..., m$ is the signal transmitted by the primary user, $s_i, i = 1, 2, ..., m$ represents the noise generated by the channel and $x_i, i = 1, 2, ..., m$ represents the signal received by the sensor.

The observed mixed signal is separated using the ICA by blind source separation. The aim of blind source separation is to find a separation matrix W, which gives an estimate Y of the source signal S from the observed signal X.

$$Y = WX = WAS. \tag{5}$$

The above equation shows that if the separation matrix W is approximated by A^{-1}, (5) can be written as

$$Y = WAS = A^{-1}AS = IS = S. \tag{6}$$

At this point, Y is approximated by the source signal S.

W can be obtained from the objective function $F(W)$. When the relevant mathematical algorithm is used to make $F(W)$ reach an optimal solution, W is then the separation matrix, and depending on the different definitions of $F(W)$, and the method of finding W, different ICA algorithms can be obtained. The ICA_p algorithm used in this paper is an ICA algorithm using Hessian approximate precoding.

The objective function used in the model is the negative mean log likelihood of the parameterization of the separation matrix $W = A^{-1}$, as follows:

$$F(W) = -\frac{1}{T}\log p(X \mid W^{-1}). \tag{7}$$

Finally, the source signal is recovered by solving for the separation matrix W when the objective function $F(W)$ reaches optimality.

III. BLIND SOURCE SEPARATION DETECTION METHOD BASED ON WAVELET TRANSFORM AND SINGULAR SPECTRUM ANALYSIS

At low SNR, the blind source separation is unsatisfactory, so the observed signal is correlated before the signal is separated.

A. DENOISING OF MIXED SIGNALS USING WT

From a signal science perspective, wavelet denoising is a

signal filtering problem, and although to a large extent wavelet denoising can be seen as low-pass filtering, it is superior to traditional low-pass filters in this respect because it also successfully retains signal features after denoising. As can be seen, wavelet denoising is actually a combination of feature extraction and low-pass filtering functions, the flow block diagram of which is shown in Fig. 1.

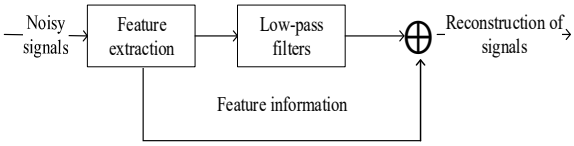

Fig.1. Block diagram of wavelet denoising

In the wireless communication environment, the white noise has the same effect on all wavelet coefficients due to the uneven spatial distribution and small wavelet coefficients, so the WT can be used to denoise the observed signal and thus improve the separation. The WT signal $X^{'}(t)$ is denoted as

$$X^{'}(t)=\left\langle X(t),\psi_{a,b}(t)\right\rangle=\int_{-\infty}^{\infty}X(t)\psi_{a,b}^{*}(t)dt=\int_{-\infty}^{\infty}\left(AS(t)+N(t)\right)\psi_{a,b}^{*}(t)dt \quad (8)$$

Where $\psi_{a,b}(t)$ is the wavelet basis and $\psi_{a,b}{}^{*}(t)$ is the conjugate of the wavelet basis. In this paper, the Daubechies wavelet is chosen as the wavelet basis because it is continuously orthogonal and it has the smallest branching.

B. THE WT SIGNAL $X^{'}(t)$ IS PROCESSED AGAIN USING SSA TO RECONSTRUCT THE SINAL

The main steps in SSA include embedding, decomposition, grouping, and reconstruction. In this paper, SSA is used to process signals because it includes singular value decomposition (SVD) as one of the steps in SSA, as SVD decomposes the signal, a process that involves reducing the dimensionality of the signal by retaining the significant components and removing the insignificant ones.

The first step is to form the trajectory matrix by lag-sorting the WT signal $X^{'}(t)$ through a suitable window length

$$X^{'}=\begin{bmatrix}x_1^{'} & x_2^{'} & \cdots & x_{T-L+1}^{'}\\ x_2^{'} & x_3^{'} & \cdots & x_{T-L+2}^{'}\\ \cdots & \cdots & \cdots & \cdots\\ x_L^{'} & x_{L+1}^{'} & \cdots & x_T^{'}\end{bmatrix}. \quad (9)$$

Where T is the sequence length and L is the window length, usually taken as $L<\frac{T}{2}$. Let $K=T-L+1$, then the trajectory matrix $X^{'}$ can be rewritten as a matrix of $L\times K$

$$X^{'}=\begin{bmatrix}x_1^{'} & x_2^{'} & \cdots & x_K^{'}\\ x_2^{'} & x_3^{'} & \cdots & x_{K+1}^{'}\\ \cdots & \cdots & \cdots & \cdots\\ x_L^{'} & x_{L+1}^{'} & \cdots & x_T^{'}\end{bmatrix}. \quad (10)$$

The trajectory matrix $X^{'}$ is then decomposed by SVD, and the resulting sequence is grouped and reconstructed.

The reconstruction requires the calculation of the projection of the hysteresis sequence $X_i^{'}$ onto U_m

$$a_i^m=X_i^{'}U_m=\sum_{j=1}^{L}x_{i+j}^{'}U_{m,j},0\le i\le T-L. \quad (11)$$

Where $X_i^{'}$ denotes the i th column of the trajectory matrix $X^{'}$, U_m is the eigenvector corresponding to the eigenvalue λ_m, and a_i^m is the weight of the time-evolving pattern reflected by $X_i^{'}$ at time $x_{i+1}^{'},x_{i+2}^{'},...,x_{i+L}^{'}$ of the original series, called the temporal principal component (TPC).

The signal is then reconstructed by means of a temporal empirical orthogonal function and temporal principal components, and the specific reconstruction process is as follows

$$x_i^{'k}=\begin{cases}\frac{1}{i}\sum_{j=1}^{i}a_{i-j}^{k}U_{k,j},1\le i\le L-1\\ \frac{1}{L}\sum_{j=1}^{L}a_{i-j}^{k}U_{k,j},L\le i\le T-L+1\\ \frac{1}{T-i+1}\sum_{j=i-T+L}^{L}a_{i-j}^{k}E_{k,j},T-L+2\le i\le T\end{cases}. \quad (12)$$

The sum of all reconstructed sequences should be equal to the original sequence, i.e.

$$x_i^{'}=\sum_{k=1}^{L}x_i^{'k},i=1,2,...,T. \quad (13)$$

C. SUBSTITUTING THE RECONSTRUCTED SIGNAL $x_i^{'k}$ INTO THE SYSTEM MODEL

To bring $x_i^{'k}$ into the system model:

$$x_i^{'k}=AS+n. \quad (14)$$

Since the signals assumed in this paper are independent of each other, the probability of A

$$p(X_i^{'k}\mid A)=\prod_{t=1}^{T}\frac{1}{|\det(A)|}\prod_{i=1}^{m}p_i([A^{-1}x_i^{'k}k]_i(t)). \quad (15)$$

Where $p_i(\cdot)$ is the i th signal probability density function.

Bringing (15) into the objective function (7), we get

$$F(W)=-\log|\det(W)|-E[\sum_{i=1}^{T}\log(p_i(y_i(t)))]. \quad (16)$$

Among them $Y=WX$.

The next solution minimizes the objective function $F(W)$ with respect to W. This corresponds to solving the ICA problem in a maximum likelihood sense. The variation of $F(W)$ with respect to W can be expressed by the Tait expansion of $F((I+\varepsilon)W)$

$$F((I+\varepsilon)W)=F(W)+\left\langle G\mid\varepsilon\right\rangle+\frac{1}{2}\left\langle\varepsilon\mid H\mid\varepsilon\right\rangle+\mathrm{O}(\left\|\varepsilon\right\|^3). \quad (17)$$

The first-order terms are controlled by matrices of order $T \times T$ and are called relative gradients. The second-order term depends on the tensor H of $T \times T \times T \times T$ and is called the relative Hessian matrix. Both of these quantities can be obtained from the second order expansions of $\log\det(\cdot)$ and $\log p_i(\cdot)$

$$\log|\det(I+\varepsilon)| = Tr(\varepsilon) - \frac{1}{2}Tr(\varepsilon^2) + O(\|\varepsilon\|^3). \quad (18)$$

$$\log p_i(y+e) = \log p_i(y) - \psi_i(y)e - \frac{1}{2}\psi_i'(y)e^2 + O(\|\varepsilon\|^3). \quad (19)$$

Where ε is a small matrix of $T \times T$ and e is a very small number. where $\psi_i = -\frac{p_i'}{p_i}$, in general, is $\tanh(\frac{\cdot}{2})$. The collection and rearrangement of a to produce the classical expression of first order

$$G_{ij} = E[\psi_i(y_i)y_i] - \delta_{ij}. \quad (20)$$

Or write it as another expression

$$G(Y) = \frac{1}{T}\psi(Y)Y^T - Id. \quad (21)$$

The second-order relative Hessian matrix can be written as

$$H_{ijkl} = \delta_{il}\delta_{jk}E[\psi_i(y_i)y_j] + \delta_{ik}E[\psi_i'(y_i)y_jy_l]. \quad (22)$$

The Hessian matrix approximation is discussed on the basis of the following moments

$$\begin{cases} \hat{h}_{ijl} = E[\psi_i'(y_i)y_jy_l] & 1 \le i,j,l \le N \\ \hat{h}_{ij} = E[\psi_i'(y_i)y_j^2] & 1 \le i,j \le N \\ \hat{h}_i = E[\psi_i'(y_i)] & 1 \le i \le N \\ \hat{\delta}_i^2 = E[y_i^2] & 1 \le i \le N \end{cases}. \quad (23)$$

Therefore, the relative Hessian matrix is

$$H_{ijkl} = \delta_{il}\delta_{jk}E[\psi_i(y_i)y_i] + \delta_{ik}\hat{h}_{ijl} \qquad i \ne j. \quad (24)$$

The first approximation of H lies in the substitution of $\hat{h}_{ijl}$ for $\delta_{jl}\hat{h}_{ij}$ and $\tilde{H}^2$ for this approximation

$$\tilde{H}^2_{ijkl} = \delta_{il}\delta_{jk}E[\psi_i(y_i)y_i] + \delta_{ik}\delta_{jl}\hat{h}_{ij} \qquad i \ne j. \quad (25)$$

The second approximation is represented by $\tilde{H}^1$, going one step further and replacing $\hat{h}_{ij}$ with $\hat{h}_i\delta_j^2$

$$\begin{cases} \tilde{H}^1_{ijkl} = \delta_{il}\delta_{jk}E[\psi_i(y_i)y_i] + \delta_{ik}\delta_{jl}\hat{h}_i\delta_j^2 & i \ne j \\ \tilde{H}^1_{ijkl} = 1 + \hat{h}_{ii} \end{cases}. \quad (26)$$

Finally, the approximate Hessian matrix is derived

$$H_{ijkl} = \delta_{il}\delta_{jk}E[\psi_i(y_i)y_j] + \delta_{ik}\delta_{jl}E[\psi_i'(y_i)], i \ne j. \quad (27)$$

Substituting (26) into (17) gives

$$\langle G \mid \varepsilon \rangle + \frac{1}{2}\langle \varepsilon \mid \tilde{H} \mid \varepsilon \rangle = \sum_{i<j}(G_{ij} - G_{ji})\varepsilon_{ij} + \frac{\hat{k}_i + \hat{k}_j}{2}\varepsilon_{ij}^2. \quad (28)$$

Where $\{\varepsilon_{ij}, 1 \le i \le j \le N\}$, $\hat{k}_i$ are defined as

$$\hat{k}_i = E[\psi_i(y_i)y_i] - E[\psi_i'(y_i)]. \quad (29)$$

When $\hat{k}_i + \hat{k}_j > 0$, so that $\varepsilon_{ij} = -(G_{ij} - G_{ji})/(\hat{k}_i + \hat{k}_j)$ minimizes (28), the resulting quasi-Newton step

$$W_{k+1} = e^D W_k$$
$$D_{ij} = -\frac{2}{\hat{k}_i + \hat{k}_j} \cdot \frac{G_{ij} - G_{ji}}{2}. \quad (30)$$

In summary, this paper uses WT and SSA to process the mixed signal, and then uses ICA_p to separate the signal after processing, the specific process is shown in Fig. 2, the specific steps are as follows.

1. Denoising of the observed signal using the WT.
2. Denoising and dimensionality reduction of the processed signal again using SSA.
3. Correlation of signal removal with whitening.
4. Separation of the signal after preprocessing using the ICA_p algorithm.

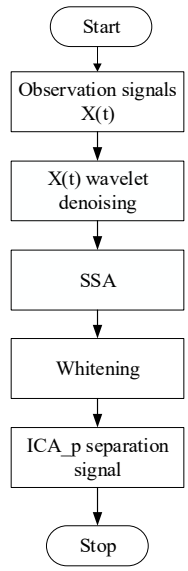

Fig. 2. Blind source separation process based on WT and SSA

IV. SIMULATION EXPERIMENTS AND ANALYSIS

To demonstrate more intuitively the process of blind source separation and spectrum analysis, the ICA_p algorithm is chosen to separate and reconstruct the signal at a SNR of 2 dB. Assuming the presence of 2 channels in the communication system and a sampling frequency f_s of 1KHz, the sampling period $t = 1/f_s$.

Fig. 3 and Fig. 4 show the time domain waveforms of the source signal, where the signal of channel 1 is $s1 = \sin(2\pi \times 20t)$ and the signal of channel 2 is $s2 = (1 + 0.5\sin(2\pi \times 5t)) \times \sin(2\pi \times 50t)$.

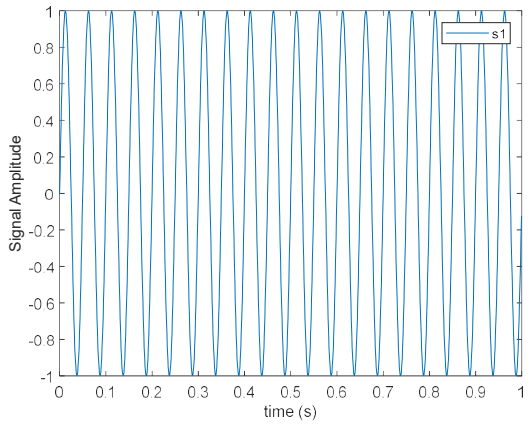

Fig. 3. Time domain waveform of source signal s1

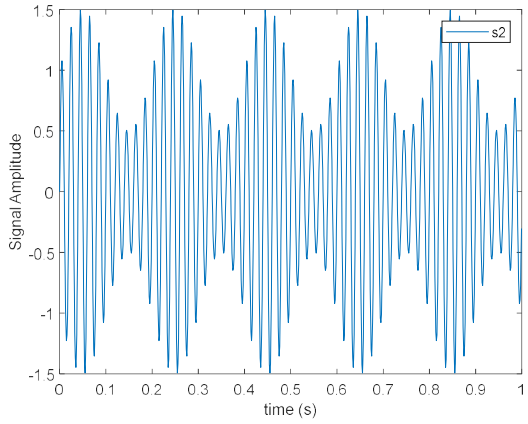

Fig. 4. Time domain waveform of source signal s2

Fig. 5 shows the spectrum corresponding to the source signal.

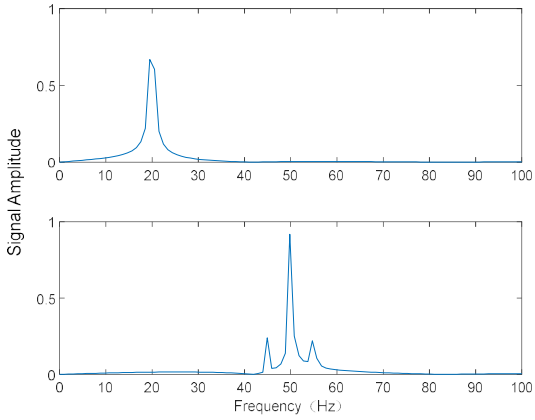

Fig.5. Source signal spectrum

In Fig. 5, it can be seen that the center frequencies of the two source signals are 20 Hz and 50 Hz, respectively.

The mixed signal obtained after the source signal has been passed through the mixing matrix is shown in Fig. 6 and Fig. 7.

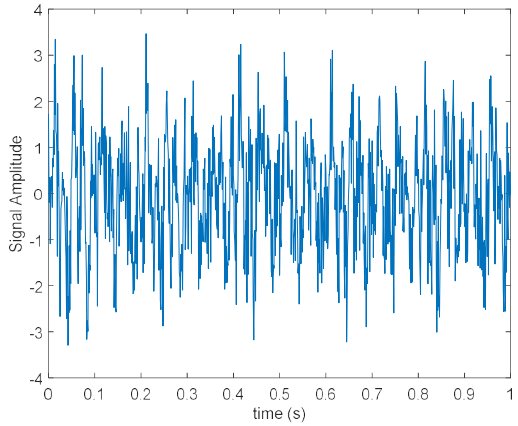

Fig. 6. Time domain waveform of mixed signal

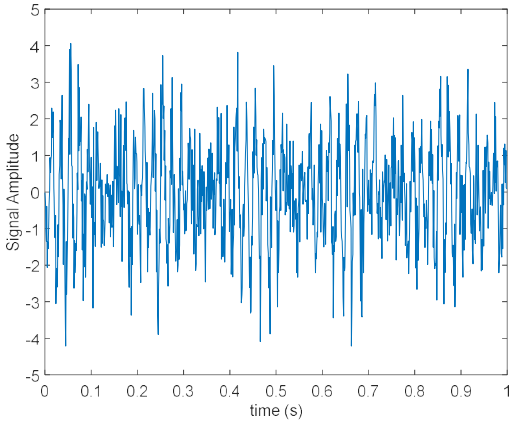

Fig. 7. Time domain waveform of mixed signal

A comparison of Fig. 3 and Fig. 4 with Fig. 6 and Fig. 7 shows that after the source signals have passed through the Gaussian channel, the waveform of the received observation signal is very different from the original signal, the waveform of the observation signal has changed due to the mixing of the signal during transmission.

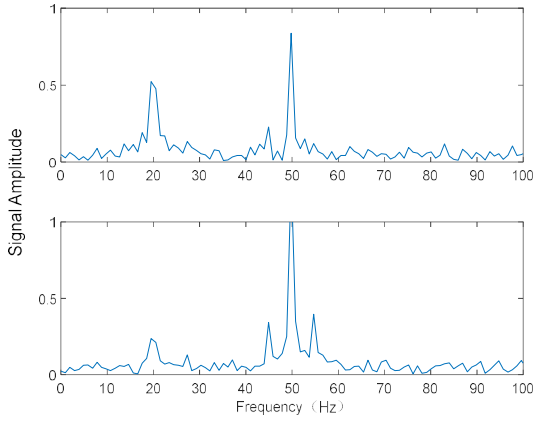

Fig. 8. Spectrogram of mixed signals

Fig. 8 shows the spectrum of the mixed signal. From Fig. 8, it can be seen that the center frequencies of signal 1 are 20 Hz and 50 Hz, and the center frequencies of signal 2 are 20 Hz and 50 Hz.

Compared with Fig. 5, it shows that the center frequency of signal 1 has not only the center frequency of the source signal of 20 Hz, but also an additional center frequency of 50 Hz, and signal 2 has a new center frequency of 20 Hz. From this result in the Fig. 8, it can be found that these source signals, after passing through the mixing matrix, produce a certain spectral overlap in the spectrum and thus it is difficult to distinguish multiple different signals through the spectrogram.

Fig. 9 and Fig. 10 show the waveforms of the signal separated from the mixed signal using the wavelet transform followed by the ICA_p algorithm.

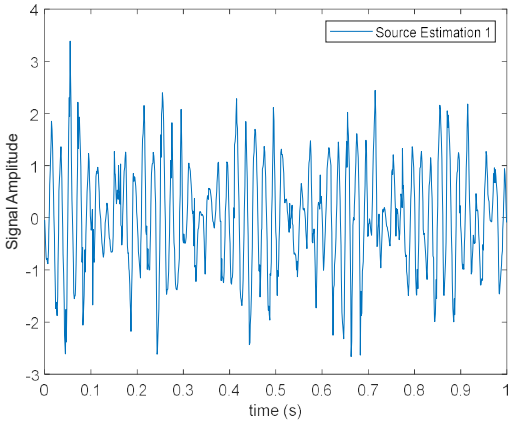

Fig. 9. WT-ICA_p separated signal waveform 1

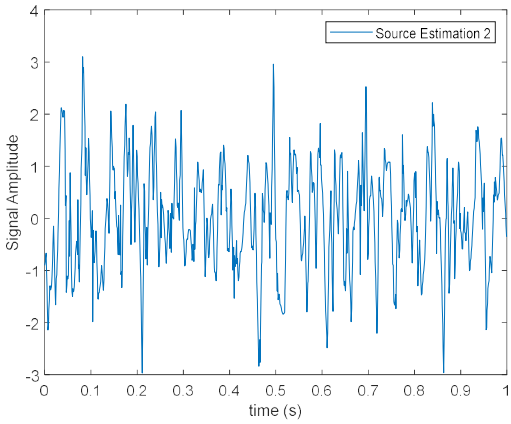

Fig. 10. WT-ICA_p separated signal waveform 2

Compared with Fig. 3 and Fig. 4, it can be found that although the WT-ICA_p algorithm is able to separate the signals, the waveforms obtained by the separation are still somewhat different from the source signals, especially the separated signal 2.

Fig. 11 shows the spectrum of the ICA_p separated signal after WT.

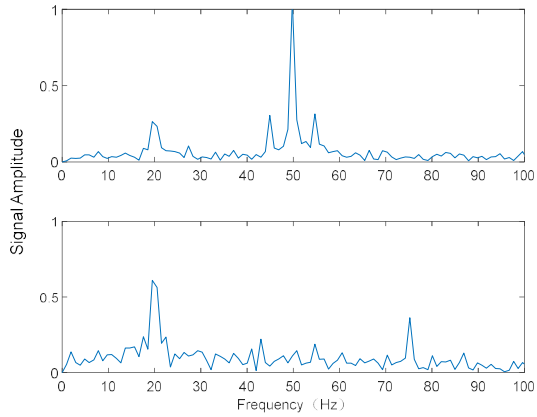

Fig. 11. Spectrum of WT-ICA_p separated signal

From Fig. 11, we can see that the center frequencies of signal 1 are 20 Hz and 50 Hz, and the center frequencies of signal 2 are 20 Hz and 75 Hz. Comparing with Fig. 5, we find that signal 1 has a new center frequency of 20 Hz and signal 2 has a new center frequency of 75 Hz, so the algorithm of separating the signals by ICA_p after wavelet transform processing is not very effective, and there is still some spectral It is also difficult to distinguish several different signals through the spectrogram.

Fig. 12 and Fig. 13 show the time domain plots after the signal has been first WT, then SSA, and finally separated using the ICA_p algorithm.

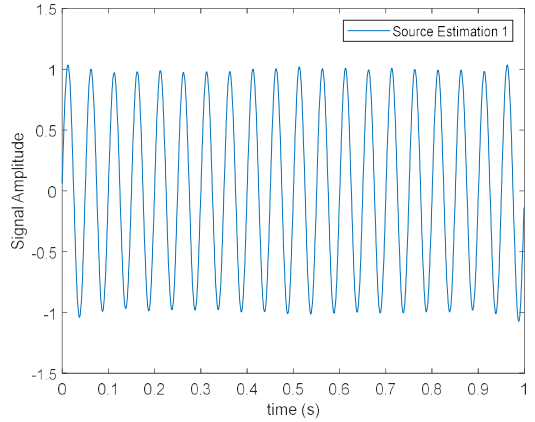

Fig. 12. WT-SSA-ICA_p separated signal waveform 1

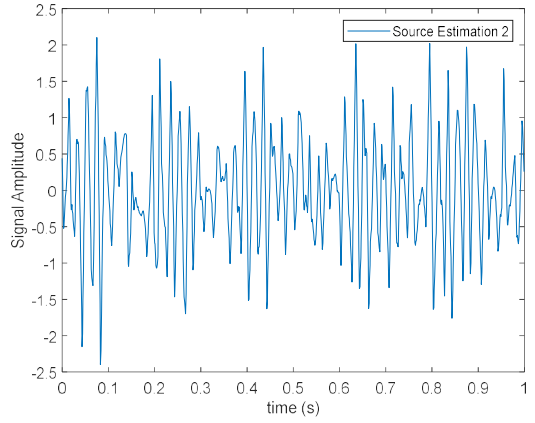

Fig. 13. WT-SSA-ICA_p separated signal waveform 2

Compared with Fig. 3 and Fig. 4, it can be found that the WT-SSA-ICA_p algorithm can separate the signals better, and the waveforms of the separated signals are basically the same as those of the source signals, indicating that the algorithm has better separation. As the signals are independent of each other, the WT is used to preprocess the signals before separation, which can effectively remove the influence of noise, and then the preprocessed signals are again processed with SSA to reduce the peace and remove noise, and finally the separation is carried out with the ICA_p algorithm, and the separation effect obtained is not disturbed by the spectral overlap, thus obtaining a waveform close to the original signal. The proposed algorithm can effectively separate these spectrally overlapped signals from their blind sources.

Fig. 14 shows the spectrum of the WT-SSA-ICA_p separated signal.

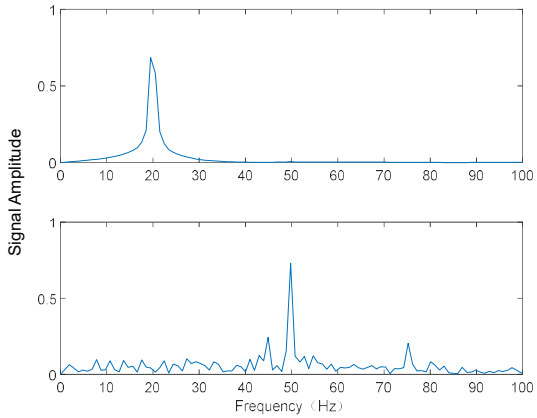

Fig. 14. Spectrum of WT-SSA-ICA_p separated signal

From Fig. 14, we can see that the center frequency of signal 1 is 20Hz, and the center frequencies of signal 2 are 50Hz and 75Hz. Comparing with Figure 4, we find that only signal 2 has a new center frequency of 75Hz, so the algorithm of separating the signals after WT processing and then using SSA and finally ICA_p works better, although only one signal 2 has spectral overlap on the spectrum, but signal 1 is very well separated and the signal can be completely distinguished from the spectrogram.

V. PERFORMANCE ANALYSIS

To evaluate the performance of the blind source separation algorithm, the correlation coefficient C is introduced as a performance indicator by comparing the similarity of the separated signal with the input signal.

$$C(x,y)=\frac{\operatorname{cov}(x,y)}{\sqrt{\operatorname{cov}(x,x)}\sqrt{\operatorname{cov}(y,y)}}. \tag{31}$$

Where $\operatorname{cov}(x,y)$ is the covariance of x and y, with the expression shown in (32).

$$\begin{aligned}\operatorname{cov}(x,y)&=E[x-E(x)]E[y-E(y)]\\&=E(xy)-2E(x)E(y)+E(x)E(y)\\&=E(xy)-E(x)E(y)\end{aligned}. \tag{32}$$

Where $E(\cdot)$ is the expected value and the correlation coefficient takes a range of $0\le C(x,y)\le 1$. When x and y are not correlated $C(x,y)$ takes 0. The closer $C(x,y)$ is to 1, the greater the correlation between x and y, and the more similar x and y are, the better the separation algorithm.

To analyze the performance of the algorithms, 3000 experiments were conducted using (31) to measure the similarity between the input source signals and the separated signals, and the average correlation coefficients of the two blind source separation algorithms were obtained, as shown in Fig. 15.

As can be seen from Fig. 15, although the correlation coefficient of the WT-ICA_p algorithm increases as the SNR increases, the correlation coefficient of the WT-SSA-ICA_p algorithm remains above 0.95 throughout and the value is very stable, which indicates that the WT-SSA-ICA_p algorithm can separate the mixed signal well and the separated signal is very similar to the source signal This shows that the WT-SSA-ICA_p algorithm can separate the mixed signal well and the separated signal is very similar to the source signal.

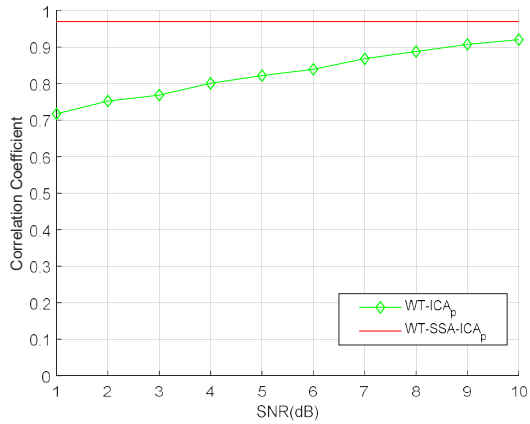

Fig.15. Correlation coefficient with SNR

It is important for communication systems to ensure the stable and reliable transmission of information. In this experimental simulation set when the correlation coefficient C is closer to 1, it is considered as a successful separation, when the value of C is too small or no solution, then the separation fails and the point is considered as a lost point, i.e. a point of nonconvergence. The probability of separation failing and the nonconvergence occurring when the two algorithms were statistically tested for 3000 trials is shown in Fig.16.

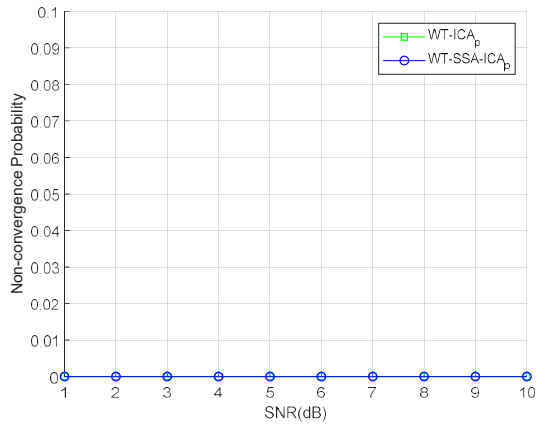

Fig.16. Variation of the probability of nonconvergence with SNR

As can be seen in Fig. 16, the results are stationary. Both

algorithms are uniform convergence regardless of the SNR change.

VI. CONCLUSIONS

In this paper, the WT-ICA_p algorithm is improved on the existing basis, i.e., the WT, by adding SSA after the WT and proposing the WT-SSA-ICA_p algorithm. Before the blind source separation, the mixed signal is first denoised with the WT, then the processed signal is denoised and reduced dimension with SSA, and finally the mixed signal is separated with the ICA_p algorithm. Then, the simulation experiments were carried out to analyze the spectrum of the signals. From the time and frequency domain plots obtained from the simulation, it can be seen that the WT-SSA-ICA_p algorithm has a better separation effect than the WT-ICA_p algorithm. Finally, the performance of the original WT-ICA_p algorithm and the WT-SSA-ICA_p algorithm is compared. The simulation results show that the two algorithms have better stability as the SNR changes, and the correlation coefficient of the WT-SSA-ICA_p algorithm is higher than that of the WT-ICA_p algorithm throughout, indicating that the WT-SSA-ICA_p algorithm can separate the mixed signals very well. The WT-SSA-ICA_p algorithm has better stability than the WT-ICA_p algorithm throughout. In the future work, the dynamic channel model and undertermined mixture model will be further considered for spectrum detection.

REFERENCES

[1] J. Ni, Z. Zhou, "Blind source separation and unmanned aerial vehicle classification using CNN with hybrid cross-channel and spatial attention module," *Scientific Reports*, vol. 15, 21905, 2025. DOI: 10.1038/s41598-025-07946-y

[2] Z. Luo, C. Li, L. Zhu, " A comprehensive survey on blind source separation for wireless adaptive processing: Principles, perspectives, challenges and new research directions," *IEEE Access*, vol. 6, pp. 66 685–66 708, 2018. DOI: 10.1109/ACCESS.2018.2879380

[3] Y. Xue, Y. Xu, A. Li, "Research on Acoustic Signal Denoising Algorithm Based on Blind Source Separation," *Procedia Computer Science*, vol. 243, pp. 380–387, 2024. DOI: 10.1016/j.procs.2024.09.047

[4] Y. Zhang, Z. Luo, "A review of research on spectrum sensing based on deep learning," *Electronics*, vol. 12, no. 21, 4514, 2023. DOI: 10.3390/electronics12214514

[5] W. Zhang, Z. Luo, X. Xiong, "Impulse noise suppression based on power iterative ICA in power line communication," *International Journal of Electronics and Telecommunications*, vol. 65, no. 4, pp. 651–656, 2019. DOI: 10.24425/ijet.2019.129824

[6] S. Basiri, E. Ollila and V. Koivunen, "Alternative Derivation of FastICA With Novel Power Iteration Algorithm," *IEEE Signal Processing Letters*, vol. 24, no. 9, pp. 1378–1382, 2017. DOI: 10.1109/LSP.2017.2732342.

[7] P. Ablin, J. F. Cardoso, A. Gramfort, "Faster independent component analysis by preconditioning with Hessian approximations," *IEEE Transactions on Signal Processing*, vol. 66, no. 16, pp. 4040–4049, 2018. DOI: 10.1109/TSP.2018.2844203

[8] G. Liu, Y. Cao, W. Feng, E. Zhao, C. Xing,"Research on adaptive threshold image denoising based on wavelet transform," *Journal of Anhui Electronic Information Vocational Technology College*, vol. 21, no. 01, pp.1–5, 2022.

[9] L. Zhao. Research on automotive noise suppression based on wavelet transform and SVD. Inner Mongolia University of Science and Technology, 2021. DOI: 10.27724/d.cnki.gnmgk.2021.000332.

[10] N. Kang, "Research on video electromagnetic leakage signal processing method based on singular spectrum analysis," *Taiyuan University of Science and Technology*, 2021. DOI: 10.27721/d.cnki.gyzjc.2021.000235.

[11] F. Xie, M. Li, J. Tian, X. Yue, Q. Yang, " A wavelet transform-based blind separation method for single-channel signals," *Modern Electronics Technology*, vol. 44, no. 07, pp. 56–59, 2021. DOI: 10.16652/j.issn.1004-373x.2021.07.011.

[12] C. Yi, W. Yuan, "Application analysis of time series models based on wavelet analysis and singular spectrum analysis," *Geomining and Mapping*, vol. 35, no. 04, pp. 6–9, 2010. DOI: 10.16864/j.cnki.dkch.2019.0050.

Qian Hu received the B S. degree in communication engineering from the Sichuan University of Science and Engineering (SUSE), Zigong, China, in 2020. She is currently pursuing the master's degree with the Sichuan University of Science and Engineering, Yibin. Her research interests include machine learning and cognitive radio.

Zhongqiang Luo received the B.S. and M.S. degrees in communication engineering and pattern recognition and intelligent systems from Sichuan University of Science and Engineering, Zigong, China, in 2009 and 2012, respectively. He received the Ph.D. degree in communication and information systems from University of Electronic Science and Technology of China (UESTC), in 2016. Since 2017, he has been with the Sichuan University of Science and Engineering, where he is currently a professor. From December 2018–December 2019, he was a visiting scholar with Department of Computer Science and Electrical Engineering of University of Maryland Baltimore County (UMBC). His research interests include spectrum sensing, blind source separation, signal processing for wireless communication system and intelligent signal processing.

Wenshi Xiao received a bachelor' s degree in elec- trical engineering and automation from the school of science and information technology of Hebei University of Engineering in 2021. Since 2021, she has been studying in Sichuan University of light and chemical technology, where she is a graduate student. Her research direction is the design of communication physical layer based on artificial intelligence.